Substituted Polyacetylenes at the Air–Water Interface

R. C. Advincula,† R. S. Duran,*,† J. LeMoigne,*,‡ and A. Hilberer‡

Center for Macromolecular Science & Engineering, Department of Chemistry, University of Florida, Gainesville, Florida 32611, and Institut de Physique et Chimie des Materiaux de Strasbourg, Groupe des Materiaux Organiques, and Institut C. Sadron, 67083 Strasbourg, France

Received September 1, 1992; Revised Manuscript Received March 9, 1993

ABSTRACT: A series of poly(*p*-ethynylbenzoate esters) synthesized using group 6 metal catalysts was investigated with respect to substituent variation and their effect on film behavior at the air–water interface. The increase in length and stiffness of the lateral substituent has the effect of decreasing the trans isomer content as well as the pure configurational sequences of the chain microstructure for this particular catalyst system. The polymers essentially retain their configuration and conformation upon formation. This has a consequence on their film behavior at the air–water interface in which only minor local conformational changes are observed using the Langmuir–Blodgett technique. The presence of a long alkyl chain length attached terminal to the substituent enhances this behavior.

Introduction

Polyacetylene has been studied to date primarily for its electrical conducting properties.[1] It is characterized by large π-electron delocalization along the backbone and as a consequence has a high molecular hyperpolarizability. Interesting nonlinear optical properties have also been observed by third harmonic generation (THG) and degenerate four wave mixing (DFWM).[2] The $\chi^{(3)}$ value of 2.7×10^{-8} esu for the oriented $(CH)_x$ prepared by the Durham method is exceptionally high.[3] However, the polymer is unstable to oxidation, insoluble, and difficult to process. Because of these reasons, much attention has been redirected to the substituted derivatives of polyacetylene:

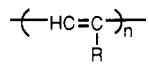

Substituted polyacetylenes are characterized by lateral substituents including heteroatoms that confer new properties on the unsaturated backbone. They are usually soluble, amorphous, or semicrystalline and are more stable to oxidation by air compared to unsubstituted polyacetylene.[4,5] The effect of the side groups is to confer these new properties but at the same time they lower the conjugation efficiency.[1] We suppose that this lower conjugation efficiency is associated with defects introduced in the polymer backbone during polymerization, e.g., saturated defects, conformational defects, etc.[6,7] A number of catalysts, reaction pathways, and different substituents studied over the years have contributed much to what we now know about these polymers. Masuda and Higashimura have published a review on the subject and have synthesized a large variety of substituents using group 5 and 6 metal catalysts.[8] A host of potential applications has been observed for these polymers ranging from materials for nonlinear optics to highly permeable gas membranes.[9,10]

Usually in a solution, flexible polymers have coiled backbones while rigid polymers are associated with rodlike geometries and poor solubility.[11] While their solution properties suggest a stiff polymer chain, substituted polyacetylenes are highly soluble and amorphous.[8] Furthermore, molecular modeling studies have indicated that the polymer conformation varies depending on the nature of the substituent group and configuration in polyacetylenes.[12] However, little systematic experimental work has been done to investigate this behavior. Recently, substituted polyacetylenes from a series of *p*-ethynylbenzoate esters with different alkyl lengths have been synthesized using the metathesis catalysts WCl_6 and $MoCl_5$ (Figure 1a).[6] The introduction of a planar ring, like a phenyl group, should increase the backbone chain stiffness and the conjugation length.[6] This has been shown by the bathochromic shifts in the UV–Vis spectra observed with phenyl-substituted polymers compared to "less bulky" alkyl groups.[7-9] However, the effect of this substitution on the polymer microstructure is unknown. Long alkyl chains should enhance solubility and give interesting relationships with the thermal transitions observed in a homologous series. They also have the ability to minimize main chain interaction thus acting as "bond solvents" to the polymer.[13]

The spreading of preformed polymers at the air–water interface to form monolayers restricts their intermolecular ordering toward two dimensions. Controlling the conformational behavior of substituted polyacetylenes confined to the air–water interface may increase the amount of conjugated segments and long range anisotropy. The conformation adopted by polymers at the air–water interface is a classical case of enthalpy minimization and entropy maximization in a system. The enthalpy of the system determines the ability of the polymer to fold or stretch out at the interface (ΔH = negative favors stretching out).[14] Temperature also has an influence especially on the entropic term ΔS. In general, as the temperature rises, the ordering effects caused by enthalpy become less significant and the disrupting effects of thermal motion become more dominant. Alternatively, the behavior can be explained as the balance between the hydration forces and the polymer–polymer interactions. Therefore, by controlling the amphiphilic nature of the polymer and the temperature, one may be able to control the conformation of the polymer in the resulting monolayer.

To date most polymers studied at the air–water interface have had flexible main chains. The backbone chain

† University of Florida.
‡ Institut C. Sadron.

0024-9297/93/2226-3895$04.00/0

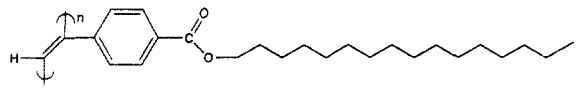

Polymer 1: poly(hexadecyl-p-ethynylbenzoate)

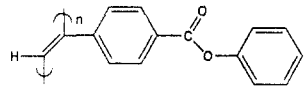

Polymer 2: poly(phenyl-p-ethynylbenzoate)

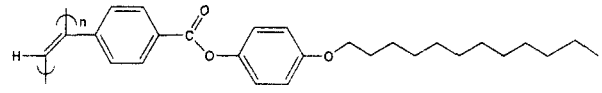

Polymer 3: poly(p'-dodecyloxyphenyl-p-ethynylbenzoate)

Figure 1. Polymer 1, poly(hexadecyl *p*-ethynylbenzoate). Polymer 2, poly(phenyl *p*-ethynylbenzoate). Polymer 3, poly(p-(dodecyloxy)phenyl *p*-ethynylbenzoate).

stiffness or flexibility also determines the packing behavior of the polymer. It has been shown that perturbation of the polymer conformation is possible with the Langmuir technique as in the case of poly-4-BCMU which exhibited a coil to rod transition leading to a red-shifted UV–Vis spectra.[15] In this study, the Langmuir film behavior of a series of substituted polyacetylenes shown in Figure 1 will be investigated at the air–water interface in order to study the effect on the local conformational behavior of each polymer with a view toward enhancing the planarity of the main chain. The semirigid nature of the double-bond single-bond polymer backbone confers unusual properties which allow the possibility of conformational changes. In the polymers studied, the stiffness and length of the lateral substituent are increased systematically by a combination of phenyl and alkyl groups. Long alkyl side chains are expected to decouple polymer–polymer interactions and thus aid in solubility. The polar carboxylic groups are expected to facilitate hydrophilic interactions with water. In principle, the right balance of substituents should give the desired monolayer behavior.

The polymers shown in Figure 1 are synthesized from a series of *p*-alkoxyphenyl esters of *p*-ethynylbenzoate prepared by using the metathesis catalyst WCl_6. These polymers were prepared in an effort to observe substituent effect on the "stiffness", microstructure, and conjugation efficiency of the polymer backbone. Comparison will be made between polymers with alkyl, phenyl, and alkoxyphenyl groups attached to the *p*-ethynylbenzoate. The synthesis and physical properties of these polymers will be described. The results will be discussed in terms of the configuration and conformation adopted by the polymer in the bulk and monolayer films. Lateral substitution is therefore expected to influence the conformation of the polymer at the air–water interface. The Langmuir technique can induce the polymeric chains to form highly ordered anisotropic films by confining them to a quasi-two-dimensional conformation. At the same time, more planar local conformation should be induced by the lateral pressure during compression and increase the conjugation length.

Results

Synthesis of Monomers and Polymers. Scheme I shows the synthetic route used for the preparation of the homologous series of *p*-ethynylbenzoate esters with *p*-alkoxyphenols of different chain lengths. The phenyl-substituted material was prepared in the same manner:[7]

Scheme I

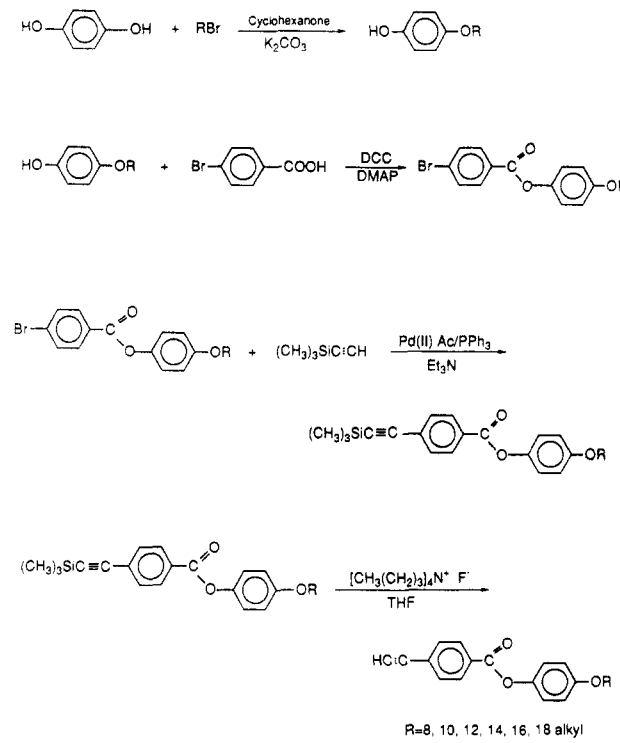

Scheme II

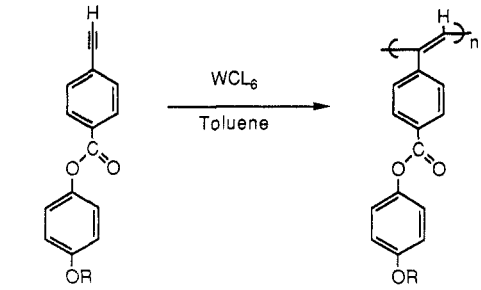

R = 8,10,12,14,16,18 R = 10,12,14

The phenols were synthesized from the base-catalyzed reaction of hydroquinone and alkyl bromide in cyclohexanone. This was followed by esterification of the purified product with *p*-bromobenzoic acid using dicyclohexylcarbodiimide (DCC) and 4-(dimethylamino)pyridine (DMAP) in methylene chloride.[16] The resulting ester was then reacted with trimethylsilylacetylene (TMSA) using a $Pd^{II}Ac/PPh_3$ catalyst system in triethylamine to produce an ethynylbenzoate derivative with a silyl group attached. The silyl group was subsequently removed by using tetrabutylammonium fluoride in THF.[17]

The purified products were yellowish solids and were soluble in a range of organic solvents depending on the alkyl chain length. Elemental analysis results were in good agreement with calculated values for the proposed structures (see Experimental Section). DSC and optical microscopy revealed no thermotropic liquid crystalline phases in all the monomers that were synthesized.

The polymerization was done with a WCl_6 metal halide catalyst in dry toluene using standard Schlenck techniques under a nitrogen atmosphere (Scheme II).[18] The same catalyst system was utilized in preparation of the other *p*-ethynylbenzoate esters shown in Figure 1a.[6] Only monomers with alkyl chains of 10, 12, and 14 carbons gave high polymeric products; the rest gave low polymerization yields. The reason for this remains unknown. The polymerization yields averaged around 90%. All the

Table I

polymer with alkyl chain (R)	molecular weight M_w[a]	polydispersity M_w/M_n	% yield
10	66 500	1.48	89
12	43 400	1.70	95
14	82 600	1.69	78

[a] Using polystyrene as a standard.

polymer obtained were highly soluble in common organic solvents such as chloroform, toluene, and THF and formed red solutions. The polymers were insoluble in methanol which was used to precipitate the product. Gel permeation chromatography using polystyrene as a standard and THF as eluent gave apparent molecular weight values summarized in Table I. Elemental analysis was in good agreement with calculated values except for the 14-carbon derivative (see Experimental Section). Since the 10- and 12-carbon chains are very similar in their structure and spectroscopic properties (only a difference of two methylene units), the data on the 12-carbon derivative will be taken as typical. The 14-carbon derivative data will not be included due to the inconclusive elemental analysis (see Experimental Section). The syntheses of polymers 1 and 2 are reported elsewhere.[6] In general, the products appeared as reddish brown amorphous solids.

Structural Characterization. The UV visible spectra of the polymers (10-, 12-, and 14-carbon derivatives) in solutions were taken using methylene chloride as solvent. A cut-off was observed at the 600-nm region and a shoulder around 450 nm for all the polymers. Polymer 3 showed two peaks at 240 and 280 nm corresponding to the phenyl group adjacent to the polymer backbone and to the alkoxy chain, respectively. For the same concentration, the p-ethynylbenzoate esters of alkyl (polymer 1) and phenyl (polymer 2) show similar spectra with higher intensities at the shoulder region and a single peak maxima at 250 nm instead.[6] For all three polymers, a transparent red film of good optical quality can be obtained by casting from a concentrated solution. No significant differences in wavelengths were observed between their solutions and cast films.

The ^{1}H NMR spectra of the 12-carbon p-alkoxyphenyl ester derivative (polymer 3) is characterized by the disappearance of the peak at 3.3 ppm (terminal acetylenic proton) and the appearance of a broad peak at 7.2–6.5 ppm corresponding to the formation of double bonds. This broad peak has been attributed to a distribution of different conformations of the cis or trans isomers and peaks of the phenylene protons.[19]

IR spectra reveals an intense absorption at the 1600-cm^{-1} region indicating the formation of double bonds. This is coupled by the disappearance of peaks at the 3300- and 2100-cm^{-1} region which are attributed to the acetylenic group of the monomer (see Experimental Section).

Figure 2 gives the ^{13}C NMR spectra of the 12-carbon p-alkoxyphenyl ester derivative. The polymer is characterized by the disappearance of the acetylenic carbons at 83 and 80 ppm compared to the monomer. The broad resonance at the 125–135 ppm region indicates the formation of the double bonds. This region is highly important for distinguishing between isomers of substituted polyacetylenes.[6,20–22] The broad peak likely arises from a distribution of conformational and configurational sequences of the polymer. Two resonances are associated with the cis and trans content of the polymer according to Percec et al.:[19] the resonances at 132 ppm are for cis and 126 for trans.

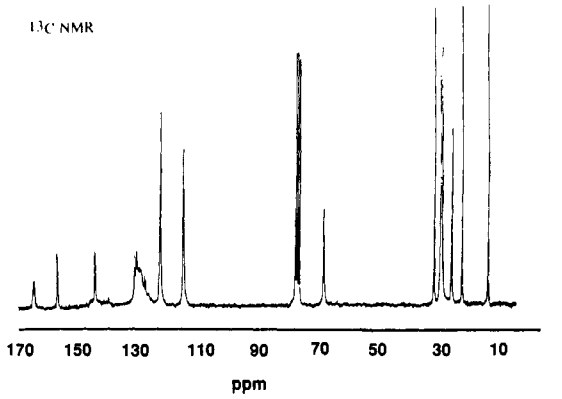

Figure 2. ^{13}NMR of poly(p-(dodecyloxy)phenyl p-ethynylbenzoate) or polymer 1 in $CDCl_3$ with a broad resonance between 125 and 135 ppm.

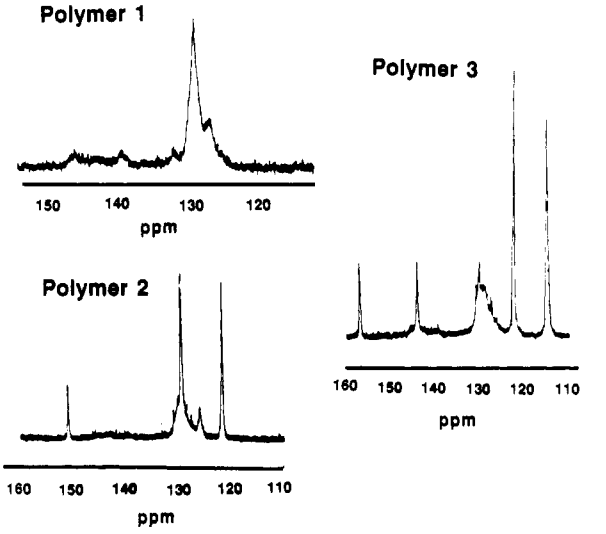

Figure 3. ^{13}C NMR of the three polymers: poly(hexadecyl p-ethynylbenzoate) or polymer 1, poly(phenyl p-ethynylbenzoate) or polymer 2, and poly(p-(dodecyloxy)phenyl p-ethynylbenzoate) or polymer 3. The resonance at 132 ppm is assigned for cis and 126 ppm for trans.

Figure 3 shows a comparison of the ^{13}C NMR spectra of the polyenic part of the three different polymers.[7] Upon close examination several important points can be observed.

First, for the alkyl derivative, the trans content at 126 ppm (tertiary carbon β to the phenyl ring), is larger than the cis. This was confirmed by observation of the resonance Raman spectra of polymer 1 at double bond stretching frequencies of 1525 and 1499 cm^{-1} (described elsewhere[6]). For the phenyl derivative, no cis peak is observed at 132 ppm, and for the alkoxyphenyl derivative, no trans or cis peaks can be clearly assigned.

Second, a broadening is observed at the 130–127 ppm region which could signify a large distribution of conformations. This distribution is a result of the nonplanar conformations adopted by the chain and the low average chain length of purely cis and trans sequences. However, the influence of the NMR relaxation time on the magnitude of this intensity is uncertain. Nevertheless, close observation of the two tertiary peaks provides a measurement of the degree of pure trans and cis sequences in the backbone. A trend toward lower content of trans sequences may be observed as substitution goes from alkyl to phenyl and alkoxyphenyl groups, presumably due to increased steric interaction. In general, this leads to a lower ratio of trans to cis content. The peak also consists of contributions from both the phenylene carbons of the

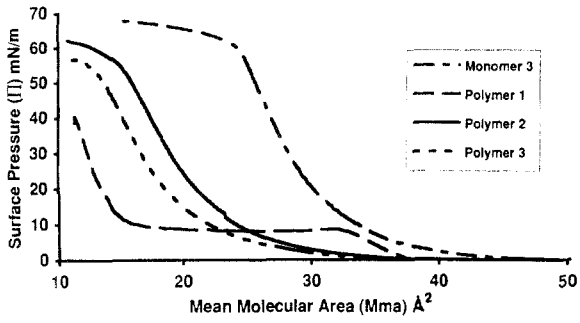

Figure 4. Surface pressure isotherms of monomer and polymers at ambient temperature compressed at a speed of 3 Å²/min.

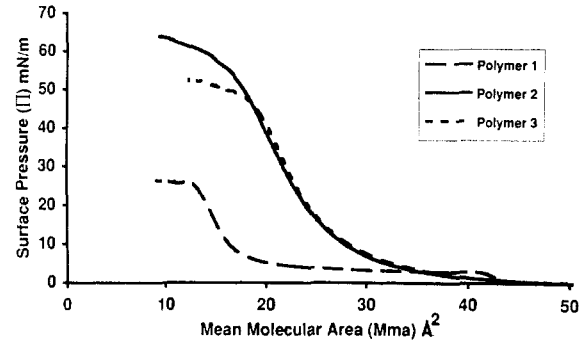

Figure 5. Surface pressure isotherms of polymers at 36 °C compressed at a speed of 3 Å²/min.

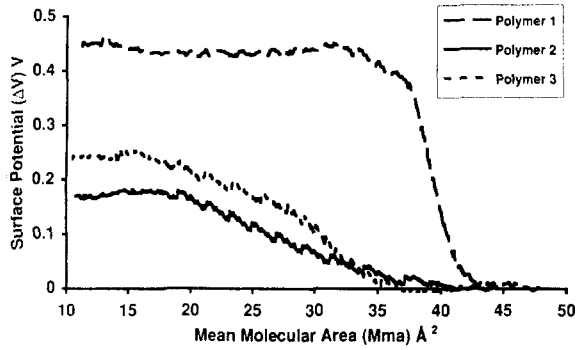

Figure 6. Surface potential isotherms of polymers at 25 °C and compressed at 3 Å²/min.

p-ethynylbenzoate as well as the ethylenic carbons of 1,3-cyclohexadiene defects.

Third, generally, the quaternary carbons have weaker signals than the tertiary carbons.[20] The resonances become weaker for the p-alkoxyphenyl derivative (polymer 3). The lack of weakness of resonances in this region is an indication of the absence of cyclohexadiene defects. Again the effect of relaxation time on the resonance intensity is uncertain. Nevertheless, this result is consistent with the decrease in the backbiting side reaction in the presence of the more sterically hindered alkoxyphenol substituent which leads to cyclohexadiene defects.[20]

DSC measurements were made on the *p*-alkoxyphenyl derivatives. These showed no transitions for chain lengths of 10 and 12 carbons. An isotropic structure was also indicated by optical microscopy measurements as a function of temperature. The DSC results indicate that these polymers are much more disordered than those with alkoxybenzoate side chains where a first-order side chain melting transition is seen for 8-carbon and 16-carbon homologues.[6]

Monolayer Studies. Isotherms. Representative isotherms of the polymers and one of the monomers are shown in Figure 4. Only the monomer of poly(p-(dodecyloxy)-phenyl *p*-ethynylbenzoate) gave a stable monolayer with an onset pressure increase at 33 Å² and a collapse pressure of 60 mN/m. The polymer has an abnormally lower limiting area (A_0) compared to its monomer. The isotherms of the phenyl (polymer 2) and alkoxyphenyl (polymer 3) derivatives are almost similar in shape and have low compressibility with an onset pressure increase at 20 and 23 Å². Polymer 1 on the other hand has an onset of 37 Å² with a plateau region between 17 and 32 Å². It exhibited a much lower collapse pressure (10 mN/m) compared to the alkoxyphenyl and phenyl derivatives which are at 55 and 52 mN/m, respectively.

Hysteresis. Measurements during compression–expansion cycles show irreversible behavior for both polymers 2 and 3.[23] Subsequent expansion and compression of their monolayers gave isotherms with little resemblance to the initial compression curve. The polymer with the alkyl chain (polymer 1) on the other hand shows a reversible behavior in the region below 10 mN/m pressure and an irreversible behavior at pressures higher than this. The polymers were subjected to different compression rates. In general, the limiting area (A_0) was observed to decrease with decreasing compression rate. This is a common behavior observed with polymers and can be attributed to relaxation at the surface with slower compression speeds.[24]

Temperature Dependence. In general, as the temperature increased, the mean molecular area (A_0) also increased. The biggest shift with temperature among the three was observed with polymer 1. The shift with polymer 3 at a higher temperature (36 °C) was significant in view of the A_0 being comparable to the value observed with the monomer at room temperature as shown in Figure 5. The collapse pressure in general decreased as the temperature increased. Only a minimal change was observed with polymer 2.

Surface Potential. The surface potential in general increased with increased compression and did not necessarily follow the curve of the isotherm as shown in Figure 6. For the series of polymers, the largest $\Delta V/$Å² was observed with polymer 1 at all temperatures. The onset surface potential rise was about 10 Å² in advance of the onset surface pressure rise. By the time the surface pressure started to increase, the rise in potential was essentially complete. Polymers 2 and 3 showed a smaller change in ΔV upon compression and have a similar behavior at different temperatures. However, with the polymer 3 surface potential diagram, a noticeable feature is the change in slope at an area of 28 Å². This does not correspond to any noticeable transition in the isotherm of the polymer.

Stability. Isobaric creep measurements done to study polymer behavior at a constant surface pressure of 5 mN/m are shown in Figure 7. Polymers 1 and 3 had a decrease in area of about 1 Å² and polymer 2 decreased by 2 Å² within 30 min. At various temperatures, the phenyl derivative showed the least deviation from this behavior while polymer 1 tended toward increased instability at higher temperatures. The polymers behaved similarly at higher surface pressures.

UV Measurements. The UV spectra of the polymers were observed in situ to determine the changes in orientation and conjugation length upon compression. Plots of the spectra are shown in Figure 8. No significant λ_{max} shift in the 300-nm region was observed for all three polymers. However, at the 450-nm shoulder, Polymer 1 showed a red shift of order 30 nm coincident with the onset rise of the surface pressure isotherm. No shifts were observed for polymers 2 and 3. To determine the relative change in intensity for the two peaks (300 and 450 nm),

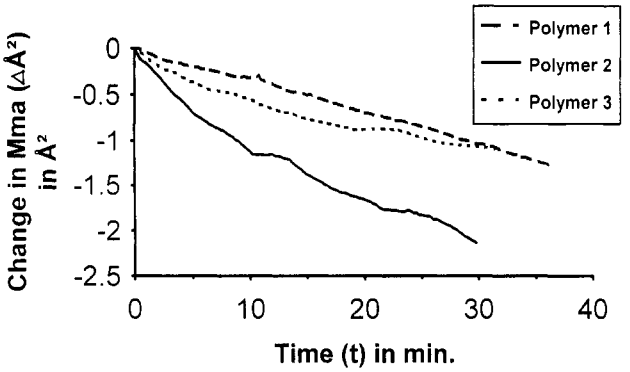

Figure 7. Isobaric creep measurements at an applied surface pressure of 5 mN/m and 25 °C.

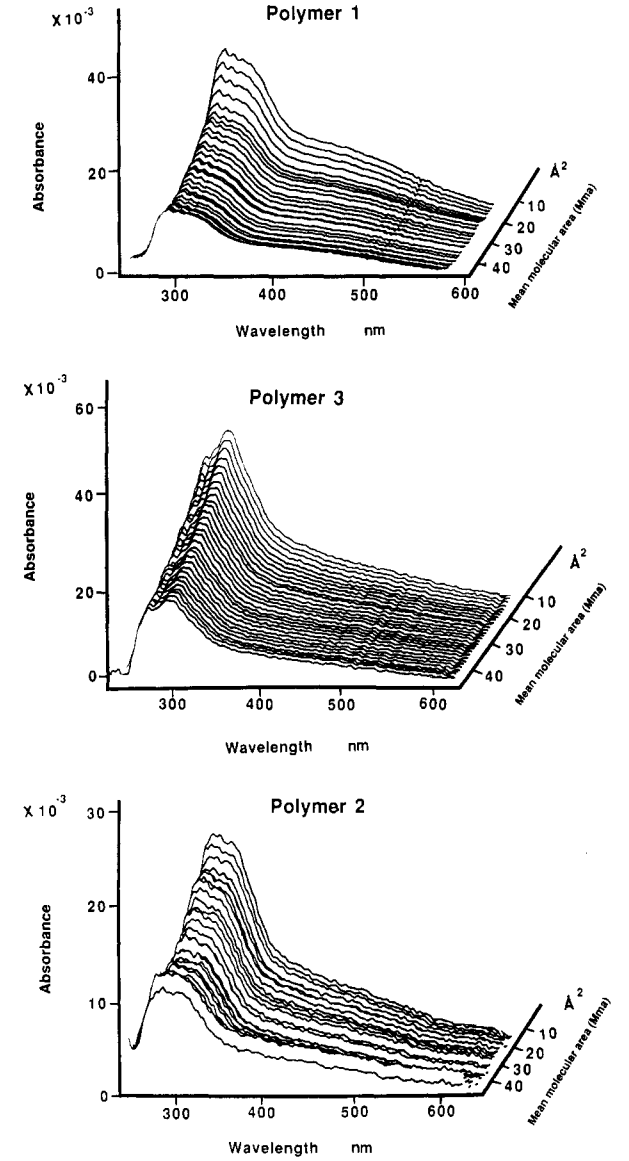

Figure 8. UV–Vis spectra of polymers at the air–water interface as a function of decreasing mean molecular area at the surface: (a, top) polymer 1; (b, middle) polymer 3; (c, bottom) polymer 2.

the ratios of their intensities were plotted as a function of change in area per molecule (Mma). The results are shown in Figure 9.

Discussion

The polymers synthesized are composed of a mixture of configurations and conformations with a higher cis ratio

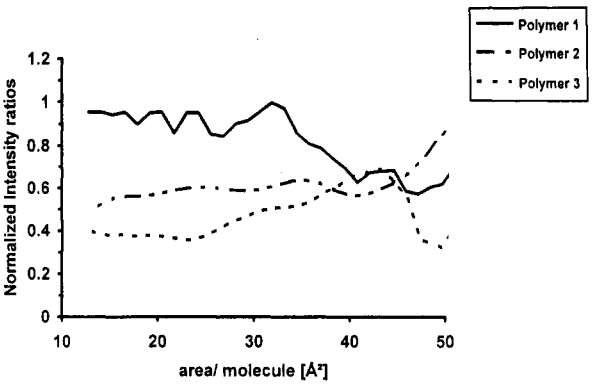

Figure 9. Change in peak intensity ratio (450 nm/300 nm) as a function of decreasing Mma.

as indicated by NMR, Raman, and IR spectroscopy.[6] Since the same catalysts and the same polymerization conditions were used for all three polymers, the above differences are clearly substituent effects. Recently, molecular mechanics and molecular dynamics calculations also indicated that the polyacetylenic backbone conformation and configuration should be substituent dependent.[12] This would mean that the size of the substituent should influence the backbone microstructure with other variables controlled.

The above effect may arise from the interaction of the substituent with the catalyst during the polymerization propagation. In a mechanism proposed by Percec,[20] the propagation occurs through a metallacyclobutene intermediate. This planar intermediate then undergoes ring scission in which the C_3–C_2 bond rotates around its axis to form a coplanar double bond. This rotation *determines* the polymer configuration. The C_3–C_2 bond will rotate in such a way that will minimize steric interaction if necessary between the substituent of the chain and the coordinated metal. Thus a cis or a trans product is obtained depending on the nature of the interaction. Because these monomers are substituted, both head-to-head and head-to-tail configurations are possible at the growing chain end. The cis or trans content may be determined by the change in conformation at the terminal repeat unit upon cleavage of the metallocyclobutene ring as shown in Figure 10. In the case of head-to-head placement, both cis or trans configurations are possible (Figure 10a). In the case of head-to-tail placement, Figure 10b indicates that the conformation resulting in trans configuration should be sterically hindered and unfavorable. Head-to-tail cis configuration is possible, however.

The above mechanism shows the effect of possible orientations and monomer placement on the growing polymer chain. Subsequent molecular geometry relaxations of the polymer would allow for changes in conformation due to rotations about single bonds. These rotations result in a planar or nonplanar conformation for a given configurational sequence. Both configurational and conformational effects could account for the broad peaks observed in the spectra. To further understand the effect of configurational sequences on planarity, molecular modeling was performed on the alkyl *p*-ethynylbenzoate polymer having an 8-carbon alkyl chain. Sequences involving head-to-head and head-to-tail placements having cis-cisoidal, cis-transoidal, trans-cisoidal, and trans-transoidal configurations were modeled. All sequences with the exception of the head-to-head trans-transoidal combination resulted in nonplanar conformations due to van der Waals interactions.[1] Figure 11 schematically shows the results obtained for the head-to-head placement trans-transoidal combination for the monomers used in this

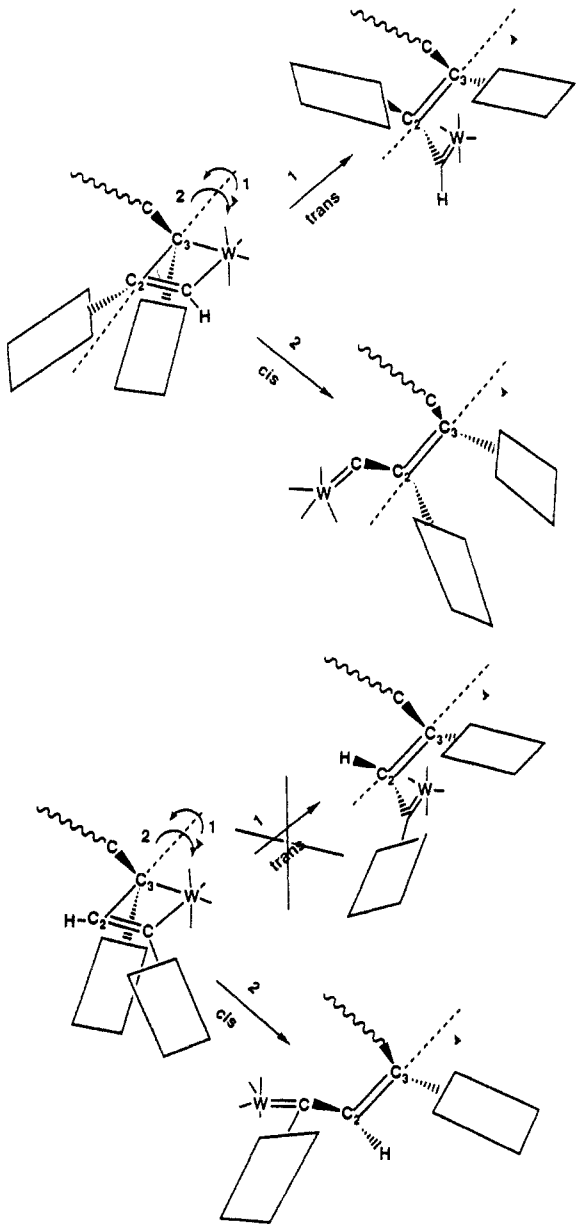

Figure 10. Mechanism of ring-opening of metallacyclobutene intermediate for substituted polyacetylenes. The top scheme (a) is for a head-to-head placement and the bottom scheme (b) for a head-to-tail placement. To simplify viewing, the polymer backbone is indicated by the bold wavy line and the lateral substituents on the terminal repeats are indicated by rectangles.

study. This can only be possible in an alternating head-to-head and tail-to-tail placement of the monomer so as to allow the proper distance between each phenyl ring and prevent steric interaction.

For the series of polymers, the effect with this particular catalyst is to decrease the trans content as the stiffness of the lateral substituent is increased. It also results in the formation of less pure configurational sequences along the series. Thus, polymerization using the metathesis catalyst WCl_6 is not specific toward formation of a highly planar chain. This implies that in order to obtain highly planar substituted polyacetylenes, a more configurationally specific catalyst than WCl_6 is needed. It also implies that the appropriate lateral substituents in the correct configuration may be an interesting means to increase the long-term conformational stability of the polyacetylene backbone.

With most polymers studied as Langmuir films, the measured Mma corresponds to the monomer repeat unit

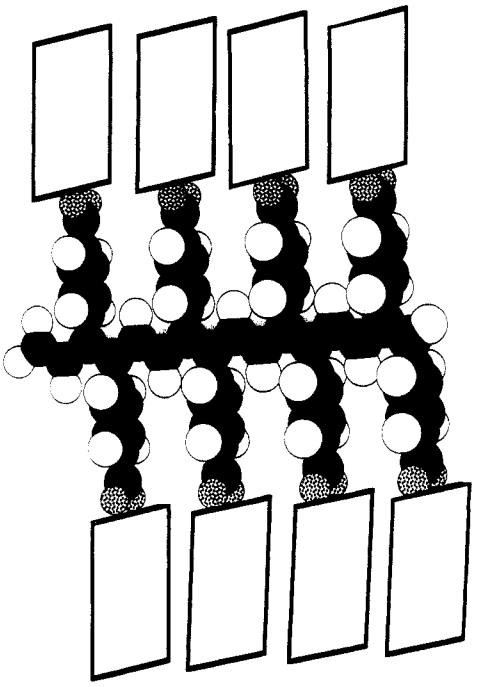

Figure 11. Space-filling model of the head-to-head trans-transoidal configuration. The lateral group adjacent to the phenyl ring is represented by a square.

area assuming that the polymer backbone lies flat on the surface with any substituents packed perpendicular to the surface (ΔH is negative).[25] With the mesogen-like substituent attached directly to the semirigid main chain, the packing of the chains will be influenced considerably by the orientation of this group. In principle, the substituents, if positioned normal to the water surface, would give low Mma, and if parallel, would give considerably higher values. This is an ideal situation wherein the main assumption is that the alkyl side chains do not affect backbone conformation considerably. As discussed above, the configuration of these polymers determined by ^{13}C NMR spectroscopy has been identified as a mixture of nonplanar cis-transoidal (or trans-cisoidal) and cis-cisoidal.[6] Small conjugated segments give rise to absorption in the visible region of the spectrum. Due to this mixture of configurations and the bulky side chains, the polymers are expected to form irregular helicoidal conformations. This would indicate that certain segments of the polymer will be out of the air–water interface as part of the helix turn.[26] As such, the polymer chains will be hindered from close packing.

In view of the lower area of the monomer compared to the polymer, the occurrence of this conformation in the monolayer is most likely. The Mma of the polymer monolayer suggests that it is neither othogonal nor flat at the interface but is in between. This means that statistically, at any given area, all the substituents are not totally adsorbed but certain segments are situated above the interface (loops).[27] Compression brings about an increase in the distribution of these loops, increasing the overfilm region which eventually lead to collapse. Thus, the polymers maintain their helicoidal and planar sequences even at the air–water interface consistent with ^{13}C NMR data in solution. Well-defined parameters such as thickness, in plane anisotropy, and periodicity of the helix turn need to be studied in order to directly define absolute conformational behavior. This can only be done with appropriate techniques, e.g., neutron reflection, X-ray fluorescence, ellipsometry, etc.[28-30] At best, only relative comparison between the conformational behavior of the

polymers can be made at this point and in the succeeding discussion.

Typical of polymer monolayers, no sharp transitions are observed with these polymers except for polymer 1. For this polymer, the reversibility of the curve before the first transition could be attributed to van der Waals interaction between the alkyl chains. This can be visualized as the side chains being lifted in or out of the water upon expansion and compression. Subsequently, the region after the first transition is attributed to a biphasic regime containing domains of close packed phenyl (stiff) parts of the substituent. The irreversibility can be explained by a rearrangement of the polymer backbone as a result of intermolecular interaction between the stiff phenyl rings directly attached to the polymer. These observations are consistent with the surface potential measurements. The surface potential curve shows a reversible behavior at pressures below the first transition and irreversibility at higher pressures. The rise in ΔV is essentially complete by the time the first transition is also finished. The slope remains flat onward, indicating the lesser role of the phenyl rings in affecting ΔV.

Polymer 3 does not have any sharp transitions in the surface pressure isotherm, but the change in slope at the surface potential diagram may reveal a stuctural transition consistent with that of polymer 1, in which the initial rise in slope can be attributed to interaction between the alkyl side chains of the polymer. Polymer 2 by comparison did not have any significant transitions in the surface pressure and surface potential isotherms. Thus, alkyl side chains influence the observed transitions in both the isotherm and the surface potential measurements depending on the proximity to polymeric backbone. The presence of a stiff phenylbenzoate substituent between the alkyl chain and the polymer decouples this effect as in the case of polymer 3.

Considering the weak hydrophilicity of the ester groups, the decay in area with time at constant pressure can be attributed mainly to a rearrangement of the phenyl and alkyl components of the substituents to accommodate the stress of compression. The stability of a monolayer is seen with a low surface area decrease over time. This is an important prerequisite for multilayer depositions (LB films) to substrates where experiments last several hours. It seems that the presence of the alkyl chain has an important role in enhancing stability possibly due to an increased intralayer van der Waals interaction. This is seen in the greater decay with time for polymer 2 which did not have any alkyl chain. However, thermal effects are in favor of the phenyl ring substituent which may have important consequences in the overall thermal stability of the polymers with time. At higher surface pressures, all the polymers show similar behavior. At this point, the backbone mobility would be primarily dependent on the stiff phenyl rings directly attached to the polymer.

Temperature dependence studies show that the shift in the mean molecular area is also dependent on the presence of the alkyl chains. The smallest variation with temperature is observed with polymer 2. The increase in Mma led to more expanded films. This would indicate increase in the surface area as a result of increased thermal motion. Significantly, the similarity in area between polymer 3 and its corresponding monomer at higher temperatures would indicate a packing arrangement approaching that of a more regular conformation. For polymer 1, the decrease in the collapse pressure and increase in onset π–A rise with increasing temperature suggests an endothermic process. This is brought about by the lowering of the energy needed to collapse the film with increasing temperature.[31]

UV measurements with the polymers at room temperature showed no significant red or blue shift at the 300-nm region with compression. Since the region at 300 nm is important for observing the presence of aggregation between the mesogen-like part of the substituent, the absence is indicative of the lack of lateral intramolecular and intermolecular ordering of the phenyl rings even with compression. This is consistent with the observed configuration by NMR in which steric interaction prevents plane stacking of the lateral substituents. At the 450-nm region, a red shift was observed for polymer 1 of the order of 30 nm while none was observed with polymers 2 and 3. This effect could be brought about by the greater amenability of polymer 1 to changes in the local conformation. The absence of a second phenyl ring lateral to the backbone gives a less stiff substituent compared to polymers 2 and 3. The presence of the alkyl chain would also allow for conformational changes due to van der Waals interactions as observed earlier with the reversibility of the surface pressure and surface potential curves.

The absorbance was observed to increase with compression for all three polymers. In order to distinguish the increases due to concentration effects from increases due to changes in local chain planarity, the ratio of peak maxima at 450 and 300 nm was taken for all the polymers. An increasing value would mean an increase in concentration of conjugated sequences in the backbone brought about by conformational changes. As shown in Figure 9, compression for polymer 1 resulted in an increase in ratio with compression leveling off at an onset coincident with that of the surface pressure isotherm. Polymer 2 showed a decreasing ratio with compression which leveled off at the onset of the surface pressure isotherm. For polymer 3, the ratio also decreased with compression but a small increase was observed prior to the onset of the surface pressure which then decreased and leveled off. These data again point to greater conformational changes associated with polymer 1 consistent with the structure. The increase with polymer 3 can be explained by the effect of the alkyl chains on the conformation of the polymers at the gaseous region. The subsequent decrease in polymer 3 as well as the decrease in polymer 2 may be due to the onset of the helicoidal conformation as discussed above. This shows that the limiting conjugation length that can be achieved is determined mainly by the type of substituent that is employed. For polymers 2 and 3 the limiting conjugation length is set at the outset of the initial polymerization conditions. Little conformational changes can be expected due to the stiff lateral substituent. For polymer 1, compression results in an increase of the conjugated sequences due to rotations on the single bonds since the phenyl substituent is not as sterically hindered as the phenylbenzoate of polymers 2 and 3. The role of the alkyl chain at the other end of the substituent can be observed for both polymers 1 and 3 as in the gaseous phase.

Thus, UV–vis absorption spectra in the monolayer indicate pressure-induced local conformational changes on segments of the backbone. These changes are highly substituent dependent. The red shift in λ_{max} at 450 nm with compression and the increase in the intensity ratio shows the importance of the lateral substituent in influencing conformational changes. Changes in local chain anisotropy will be investigated in the future using cross-polarizers with the UV–Vis spectra measurements.

Conclusion

The different substituents played an important role in determining the local conformational behavior of the polymers and their chain microstructure. The higher cis ratio is a consequence of a substituent effect and the type of catalyst used. The results show that the trans-transoidal, head-to-head placement combination, is the only configuration capable of giving substituted polyacetylenes free from steric interaction between the substituents. Regiospecific catalysts (as alternate mechanisms to chain addition) should play an important role in achieving this configuration in the synthesis of these polymers. During formation, the polymers essentially retain their configuration and conformation. The substituents are "locked in" the backbone conformation, the degree of which is dependent on the stiffness of the substituent and presence of flexible side chains. Procedures such as the Langmuir monolayer technique result in additional minor conformational changes. It is clear that all synthetic efforts on this class of polymers should be directed toward this configuration in order to optimize main chain planarity.

Experimental Section

Materials and Instrumentation. All the starting materials and solvents for the synthesis were obtained from Aldrich and were used as received. ^{13}C NMR and ^{1}H NMR spectra were recorded on a Bruker AC200F spectrometer operating at (^{1}H) 200 and (^{13}C) 60 MHz. Deuterated $CHCl_3$ was used as solvent for the measurements. Infrared spectra of the powder pressed pellets in KBr were recorded on a Perkin-Elmer 983. UV spectra were recorded on a Perkin-Elmer UV/VIS/NIR Lambda 9 spectrophotometer in Spectrograde methylene chloride, THF in solution, and on a quartz plate for the cast film. Differential scanning calorimetry was performed on a Perkin-Elmer DSC4 in aluminum pans with a heating and cooling rate of 20 °C/min. Optical observations were obtained with a Leitz Orthoplan polarizing microscope equipped with a Mettler FP52 hot stage.

The behavior of the monolayers was investigated using a KSV 5000 Langmuir–Blodgett System (KSV Instruments). The Wilhelmy plate method was used to measure the surface pressure. Surface potential measurements were done using the vibrating plate method. A PTFE trough and nylon barrier were used to compress the monolayers at a typical speed of 20 mm/min. Water for the subphase was purified to 18 MΩ using a Milli-Q water system (Millipore). The temperature of the subphase was controlled by circulating fluid from a constant temperature bath through channels cut in the trough base. The lowest subphase temperatures were obtained by prechilling the subphase water in an ice bath. A microsyringe (Hamilton) was used for spreading dichloromethane solutions of the polymers. Throughout the text and figures, surface areas are expressed per monomer repeat unit. UV measurements of monolayers on the trough were made with a modified Oriel Instaspec III equipped with a cooled photodiode array detector. Gratings of 2400 and 400 were used at their corresponding Blaze wavelengths. A scanning frequency and integration time of 1 spectra/10 s and 1 s, respectively, were used for the measurements.

Typical Synthesis of the Monomer. A mixture of the alkyl bromide (16 mmol), the hydroquinone (32–64 mmol), and potassium carbonate (64 mmol) was refluxed for 16 h in cyclohexanone. The reaction solution was filtered. The filtrate was concentrated and then recrystallized from ethanol to yield the *p*-alkoxyphenol.[32]

The esterification of the *p*-bromobenzoic acid and the *p*-alkoxyphenol was carried by dehydrating condensation using DCC.[33] To 8 mmol of *p*-alkoxyphenol in 40 mL of methylene chloride with 100 mg of DMAP was added 8 mmol of 1,4-bromobenzoic acid. The solution was initially stirred at 0 °C to which DCC was slowly added and urea precipitated. The mixture was stirred at 20 °C for 3 h and the precipitated urea filtered off. The filtrate was evaporated under vacuum and the residue was redissolved in methylene chloride in order to filter the insoluble urea. The organic solution was successively washed with aqueous solutions of HCl, $NaHCO_3$, and pure water, and finally dried. The solvent was removed and chromatography of the residue was done on a SiO_2 column with $CHCl_3$ as eluent. Crystallization in methanol/methylene chloride gave white platelets of the esterified product.

Table II

alkyl chain length of derivative	%C, %H, %O	
	Calculated	Observed
8	78.9, 7.4, 13.7	78.6, 7.6, 13.8
10	79.4, 7.9, 12.7	79.1, 8.0, 12.9
12	79.8, 8.4, 11.8	79.8, 8.5, 11.7
14	80.2, 8.7, 11.1	79.2, 8.8, 12
16	80.5, 9.1, 10.4	81.1, 12.18, 6.72
18	80.8, 9.4, 9.8	78.9, 9.3, 11.8

The bromo derivative was then reacted with trimethylsilylacetylene (TMSA) to subsequently produce an ethynylated product.[34] To a dearated solution of the (17 mmol) bromo derivative in 50 mL of anhydrous triethylamine, 34 mmol of TMSA was added dropwise. Catalyst palladium(II) acetate (5 mg) was then added together with 50 mg of triphenylphosphine. The mixture was refluxed for 24 h, then cooled and filtered to remove the hydrobromide salt. The orange-brown filtrate was concentrated, mixed with 200 mL of aqueous sodium bicarbonate, and then extracted with dichloromethane (3 × 50 mL). The organic fractions were combined, dried over magnesium sulfate, and concentrated to yield an oil. The residue was taken up in methylene chloride and passed through a column of silica with a mixture of methylene chloride and pentane. The eluent was concentrated and further purified by column chromatography. The final product was a yellowish solid.

***p*-(Decyloxy)phenyl *p*-Ethnylbenzoate**: Yellowish solid, yield = 78%; mp 74.35 °C; IR (KBr pellet) 3240 cm^{-1} (m, sharp, acetylenic C–H stretching), and 610 cm^{-1} (m, acetlyenic ≡C–H bending), 1740 cm^{-1} (s, carbonyl ester); ^{1}H NMR ($CDCl_3$) 3.25 ppm (s, acetylenic proton), 8.2–7.6 ppm (s, 4 H aromatic benzoate), 7.2–6.9 (s, 4 H, aromatic phenol). ^{13}C NMR ($CDCl_3$) 80 and 88 ppm (acetylenic α and β), 164.88 ppm (m, carbonyl carbon), 157–115 ppm (m, 8C aromatic). Anal. Calcd: C, 78.9; H, 7.4; O, 13.7. Found: C, 78.6; H, 7.6; O, 13.8.

All monomers gave similar NMR, IR, and UV spectral observations except in the alkyl region. Elemental analysis data are summarized in Table II.

Typical Polymerization. Monomer (250 mg) and catalyst (5.8 mg) were placed in a clean and dry reaction vessel under argon.[6] Fresh dry solvent was introduced to the reaction vessel by evaporation to make an approximately 1.0 M solution. The polymerization was carried out at 30 °C for 24 h. The product was recovered in methylene chloride and poured into a large excess (150 mL) of methanol. The precipitant was then redissolved in THF and passed through a silica column to remove the catalyst. The eluent was then concentrated and reprecipitated in methanol and then oven-dried and weighed.

Polymer of *p*-(Decyloxy)phenyl *p*-Ethynylbenzoate. A reddish brown product was obtained with 89% yield. IR (KBr) 1600 cm^{-1} (m, sharp polyenic double bonds), 1265 cm^{-1} (=C—H in plane deformation), disappearance of 3240-cm^{-1} peak (acetylenic C—H stretching), 922 and 970 cm^{-1} (=C—H out of plane deformation); ^{1}H NMR ($CDCl_3$) disappearance of 3.25 ppm resonance (s, acetylenic proton), 7.2–6.5 ppm (b, ethylenic protons); ^{13}C NMR disappearance of 80.4 and 82.7 ppm (acetylenic α and β), 135–125 ppm (b, ethylenic carbons with phenylene and cyclohexadiene C=C carbons). Anal. Calcd: C, 79.2; H, 8.1. Found: C, 79.1; H, 8.1.

The polymer with a 12-carbon derivative gave similar NMR, IR, and UV spectral observations except for the alkyl region. The ^{13}C NMR of the 14-carbon derivative showed a small resonance at 0.2 ppm signifying the presence of the trimethylsilyl groups in the polymer. This residue came from the incomplete conversion of the monomer by the removal of the trimethylsilyl protecting group. This could account for the discrepancy between the calculated and observed value in the elemental analysis. Despite drying of the polymer for a long time, this peak was not

removed and therefore is attached to the polymer backbone (trimethylsilane or trimethylsilylacetylenes are volatile). This would mean that some disubstituted acetylenes were copolymerized with the monomer resulting in a more irregular polymer. Some saturated defects are observed in the 4.1–3.5 ppm region in the ^{1}H NMR and between 60 and 30 in the ^{13}C NMR. This derivative was not used for comparison with the other polymers.

Acknowledgment. We acknowledge Ms. Laurence Oswald for technical assistance and Mr. Benoit Heinrich for the alkoxyphenols used in the synthesis (IPCMS, Strasbourg). This work was partly supported by Analatom, Inc., Contract No. 91-C-5654, subcontract to Analatom's SBIR contract with the Materials Laboratory Wright Patterson Air Force Base, Dayton, OH. We also acknowledge technical support from KSV Instruments, Helsinki, and Oriel Corp., Connecticut.

References and Notes

(1) Chien, J. *Polyacetylene*; Academic Press: Orlando, FL, 1984.
(2) Drury, M. *Solid State Commun.* **1988**, *68*, 417–420.
(3) Brown, C.; Vickers, P.; Foot, P.; Billingham, N.; Calvert, P. *Polymer* **1986**, *27*, 1719.
(4) Masuda, T.; Tsuchihara, K.; Higashimura, T. *J. Polym. Sci., Part A: Polym. Chem.* **1991**, *29*, 471–478.
(5) Zhang, X.; Ozcayir, Y.; Feng, C.; Blumstein, A. *Polym. Prepr.* **1990**, *31*, 597–598.
(6) LeMoigne, J.; Hilberer, A.; Strazielle, C. *Macromolecules* **1992**, *24*, 6705.
(7) LeMoigne, J.; Hilberer, A.; Kajzar, F. *Makromol. Chem.* **1991**, *192*, 515.
(8) Masuda, T.; Higashimura, T. *Adv. Polym. Sci.* **1987**, *81*, 121.
(9) Neher, D.; Wolf, A.; Bubeck, C.; Wegner, G. *Chem. Phys. Lett.* **1989**, *163*, 116–122.
(10) Masuda, T.; Higashimura, T. *J. Am. Chem. Soc.* **1983**, *105*, 7473.
(11) Elias, H. G. *Macromolecules*; Plenum Press: New York, 1984.
(12) Clough, S.; Sun, X.; Tripathy, S.; Baker, G. *Macromolecules* **1991**, *24*, 4264–4269.
(13) Ballauf, M. *Angew. Chem.* **1989**, *28*, 253.
(14) MacRitchie, F. *Chemistry at Interfaces*; Academic Press, Inc.: San Diego CA, 1990; p 17.
(15) Biegajski, J.; Burzynski, R.; Cadenhead, D.; Prasad, P. *Macromolecules* **1986**, *19*, 2459–2461.
(16) Neises, B.; Steglich, W. *Angew. Chem., Int. Ed. Engl.* **1978**, *17*, 522.
(17) Austin, W.; Bilow, N.; Kelleghan, W.; Lau, K. *J. Org. Chem.* **1981**, *46*, 2280–2286.
(18) Masuda, T.; Hasegawa, K.; Higashimura, T. *Macromolecules* **1974**, *7*, 728.
(19) Simionescu, C.; Percec, V.; Dumitrescu, S. *J. Polym. Sci., Polym. Chem. Ed.* **1977**, *15*, 2497.
(20) Sanford, T.; Allendor, R.; Kang, E.; Ehrlich, P. *J. Polym. Sci., Polym. Phys. Ed.* **1980**, *18*, 2277.
(21) Percec, V.; Rinaldi, P. *Polym. Bull.* **1983**, *9*, 548.
(22) Furlani, A.; Napoletano, C.; Russo, M.; Feast, W. *Polym. Bull.* **1986**, *16*, 311.
(23) Gaines, G. L. *Langmuir* **1991**, *7*, 834–839.
(24) Gaines, G. L. *Insoluble Monolayers at Liquid-Gas Interfaces*; Wiley Interscience: New York, 1966.
(25) Crisp, D. *J. Colloid Sci.* **1946**, *1*, 49, 161.
(26) Danielli, J. F.; Rosenberg, M. D.; Cadenhead, D. A. *Progress in Surface and Membrane Science*; Academic Press: New York, 1973.
(27) Kawaguchi, M.; Sano, M.; Chen, Y.; Zografi, G.; Yu, H. *Macromolecules* **1986**, *19*, 2606.
(28) Rennie, A.; Crawford, R. J.; Lee, E. M.; Thomas, R. K.; Crowley, T. L.; Roberts, S.; Qureshi, M.; Richards, R. *Macromolecules* **1989**, *22*, 3466.
(29) Sansone, M.; Rondelez, F.; Peiffer, D.; Pincus, P.; Kim, M.; Eisenberger, P. *Phys. Rev. Lett.* **1985**, *54*, 1039.
(30) Kawaguchi, M.; Nagata, K. *Langmuir* **1991**, *7*, 1478–1482.
(31) Matuo, H.; Rice, D.; Balthasar, D.; Cadenhead, D. *Chem. Phys. Lipids* **1982**, *30*, 367.
(32) Vogel, A. *Textbook of Practical Organic Chemistry*; 4th ed.; Longman: Essex, 1986.
(33) Neises, B.; Steiglich, W. *Angew. Chem., Int. Ed. Engl.* **1978**, *17*, 522.
(34) Austin, W.; Bilow, N.; Kelleghan, W.; Lau, K. *J. Org. Chem.* **1981**, *46*, 2280–2286.